Design and Analysis of a Four-Pendulum Omnidirectional Spherical Robot

Brian P. DeJong, Ernur Karadogan, Kumar Yelamarthi & James Hasbany

Journal of Intelligent & Robotic Systems
with a special section on Unmanned Systems

ISSN 0921-0296

J Intell Robot Syst
DOI 10.1007/s10846-016-0414-4

Springer

J Intell Robot Syst
DOI 10.1007/s10846-016-0414-4

Design and Analysis of a Four-Pendulum Omnidirectional Spherical Robot

Brian P. DeJong · Ernur Karadogan · Kumar Yelamarthi · James Hasbany

Received: 26 April 2016 / Accepted: 21 August 2016

Abstract This paper presents the design, analysis, and comparison of a novel four-pendulum spherical robot. The proposed mechanism rolls omnidirectionally via four tetrahedrally-located pendulums that shift the robot's center of mass to create rolling torque. The nine dynamic equations of motion are derived via the Lagrangian and nonholonomic constraint equations, and then simulated numerically; results show successful propulsion with expected behaviors. The mechanism is then compared to existing center-of-mass designs in terms of directionality, drive torque arm, and inertia eccentricity. In these regards, the four-pendulum design is a balance of existing designs: it is omnidirectional with eccentricity and torque capability that are in the middle of the range exhibited by existing designs. In addition, the new four-pendulum mechanism has been built and tested as a successful proof-of-concept prototype.

B. P. DeJong (✉) · E. Karadogan · K. Yelamarthi · J. Hasbany
Central Michigan University, Mount Pleasant, MI 48859, USA
e-mail: b.dejong@cmich.edu

Ernur Karadogan
e-mail: ernur.karadogan@cmich.edu

Kumar Yelamarthi
e-mail: kumar.yelamarthi@cmich.edu

James Hasbany
e-mail: hasba1jh@cmich.edu

Keywords Spherical robot · Dynamics · Center-of-mass · Nonholonomic

1 Introduction and Related Work

Remotely controlled mobile robots continue to become more popular in society and in the research literature. One interesting vein of research is in the use of spherical robots – mobile robots with an outer spherical shell that traverse an environment by rolling. These ball-shaped robots are intriguing because they move without any externally visible mode of propulsion and must navigate the nonholonomic ball-and-plane workspace. Thus, they require relatively novel motion mechanisms, subtly complex dynamic analysis, and advanced control algorithms [1–3]. No single propulsion scheme has emerged clearly better than the others, and so new mechanisms continue to be presented. Because of their outer shell, spherical robots have the advantages of being durable, non-tippable, and capable of being fully sealed from the outside environment. They have found broad applications in patrol and surveillance [4], extraterrestrial exploration [5], environmental monitoring [6], underwater [7], and even child-development [8].

This paper presents a novel spherical robot design that uses four internal pendulums for propulsion. As such, it is omnidirectional (it can roll in any direction instantly) unlike most of the existing spherical robot designs, and yet comparably agile. Here, the

Published online: 15 September 2016

design is described and implemented on a physical prototype as a proof of concept. The mechanism's dynamics are analyzed from first principles, and its motion is numerically simulated. The design is also analyzed and contrasted with existing designs in terms of directionality, torque arm, and inertia eccentricity.

Spherical robots can be roughly categorized by their drive mechanism. One technique uses conservation of angular momentum by having one or more internal flywheels that are tilted to induce rolling of the sphere. For example, Bhattacharya and Agrawal [9] use two perpendicular rotors, while Joshi and Banavar [10] use four rotors to achieve omnidirectionality. Gajamohan et al. [11] use three rotors in a cube robot to rotate and balance omnidirectionally. These robots have the advantage of being able to produce drive torques higher than pendulum designs (i.e., torque arms are greater than the sphere's radius) but the disadvantages of large internal energy and undesired precession torques.

A few spherical robots move by distorting or transforming their outer shell, or by simply using the environment's wind similar to tumbleweed. Sugiyama et al. [12] use shape-memory alloy to deform and roll wheels and spheres, while Wait et al. [13] and Artusi et al. [14] deform panels on a robot's shell via air bladders and dielectric actuators, respectively.

The most common propulsion scheme, however, is to internally change the robot's center of mass to induce rolling. This scheme has the advantage of actuation simplicity, but the disadvantage of limiting the maximum torque arm to less than the sphere's radius. There are several approaches to modifying the center of mass, as described below.

One proposed but under-studied design [15] uses a single internal mass that is hung and moved by several cables and pulleys. This design has the advantage of minimal static mass (i.e., almost all of the mass can be clustered in the movable mass), but its torque arm is limited by the locations of the cables – the mass cannot move past the bisection line from one cable mount to another.

A more common center-of-mass technique is to use an internal car or drive unit that rolls on the interior of the shell, similar to a hamster in a hamster wheel. For example Halme et al. [16] present a spring-loaded unicycle drive unit, while Bicchi and colleagues [17], and later Alves and Dias [18], use a small internal car. These designs have the advantage of well-studied drive mechanisms and result in a sphere that can roll in any direction, but are usually not instantaneously omnidirectional, as the drive unit must turn before climbing the shell. They also suffer from the typical grip-wear tradeoff of friction drives – to get good traction, the drive wheels need large normal forces, but this increases steering friction and wear.

The most common center-of-mass design is a single internal pendulum that can rotate about a main rolling axis and tilt to induce steering when rolling. For example, Seeman et al. [4] and Michaud and Caron [19] present single pendulum designs and applications. Schroll [20] analyzes and simulates the single-pendulum dynamics, while Hogan et al. [5] discusses a robot that uses a hanging payload as the pendulum. Designs also exist with two hanging pendulums and stick-slip spinning, such as Ghanbari et al. [21] and Yoon et al. [22]. The single-pendulum design has the advantage of a simple (typically two-degree-of-freedom) drive mechanism; its primary disadvantage is that it is not omnidirectional – single-pendulum designs are more "steered wheel" than "rolling sphere" because of their main drive axis. When facing forwards, for instance, these designs cannot roll purely sideways.

Alternatively, some spherical robots move the center of mass by sliding multiple masses along internal tetrahedral spokes. As the masses slide along their rail, the center of mass changes and the sphere rolls. Javadi and Mojabi [23], Sang et al. [24], and Tomik et al. [25] present such designs. These robots are omnidirectional instantaneously, but suffer from reduced torque arms since the masses cannot all converge on the ideal center-of-mass location. For example, when rolling forward, one or more distributed masses may be restricted to a backwards spoke and thus reduce rolling torque.

2 Four Pendulum Design

The spherical robot presented here uses four tetrahedrally-located pendulums to change the robot's center of mass and thus roll the sphere. The mechanism, shown in Fig. 1, includes four pendulums that rotate about the four tetrahedral axes. Their configuration (rotating about tetrahedral axes versus inline) and location (radial distance to motor, r_m and pendulum rod length, r_p) are optimized for maximum

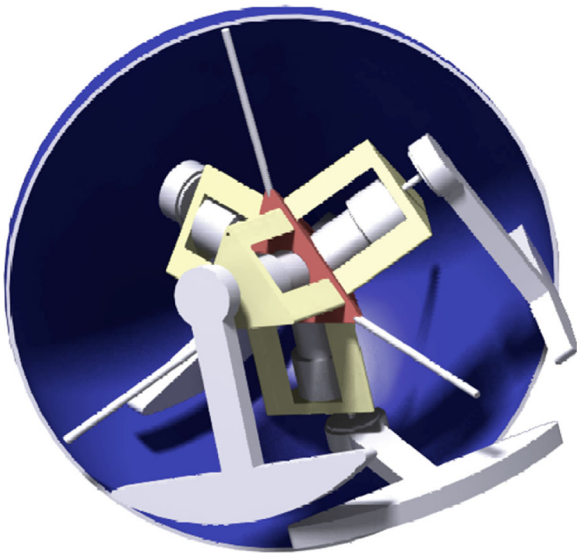

Fig. 1 CAD representation of four-pendulum mechanism

center-of-mass envelope without risking pendulum overlap. Conceptually, this location is such that the four pendulum's arcs touch at the outer shell. From rest, the mechanism can apply rolling torque in any direction instantly, and in practice, the pendulums are rotating in full circles as the robot rolls.

The mechanism has been implemented in a proof-of-concept prototype, shown in Fig. 2. The electronics and batteries are housed in a rapid-prototyped tetrahedral box in the center of a 33-cm-diameter plastic shell, with motors mounted on the box facing outwards. The robot uses a Maple r5 microprocessor, Futaba 75 MHz RF transmitter and receiver, and LiPo batteries for the motors (11 V) and electronics (3.7 V). The motors are Polulu 12V brushed DC with built-in 50:1 gear reduction and 3200 CPR-output encoders. For orientation sensing, the robot uses a CHRobotics CHR-UM6 six-axis orientation sensor that incorporates accelerometer, rate gyro, and magnetic sensor information.

The prototype successfully rolls in any direction, as commanded by the user. As an initial prototype, it is not optimized for minimum static mass nor does it include position feedback. It has a static mass of 2.6 kg with a dynamic mass of 1.6 kg; the dynamic-to-static mass ratio could be greatly improved in future prototypes. The four-pendulum configuration allows for ideal (point-mass) pendulum rod lengths of 13.5 cm in a 33 cm shell; the actual pendulums have effective lengths of 10.0 cm. Initial tests show that the prototype can accelerate with 0.6 m/s^2 and achieve a maximum speed of 0.7 m/s. The prototype proves feasibility of the four-pendulum design and allows for future testing.

3 Mechanism Dynamics

3.1 Kinematics

To describe the dynamics of the four-pendulum mechanism, we define six inertial frames: a static World frame, a Body frame centered on the sphere's center of mass, and four pendulum frames (numbered 1 to 4) centered on the corresponding pendulum's center of mass. The mechanism and frames are sketched in Fig. 3.

The Body frame rotates in the World frame using z-x'-z" intrinsic Euler notation with angles ϕ, θ, and ψ, and translates with x and y. For simplicity, the frame is assumed to also be at the sphere's geometric center such that it does not translate in the vertical direction.

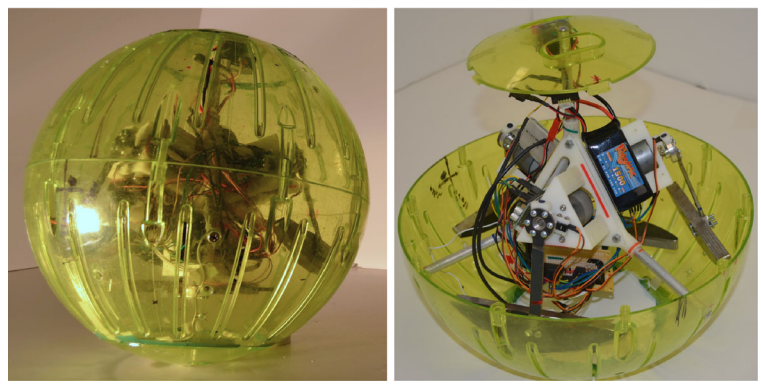

Fig. 2 Four-pendulum robot prototype

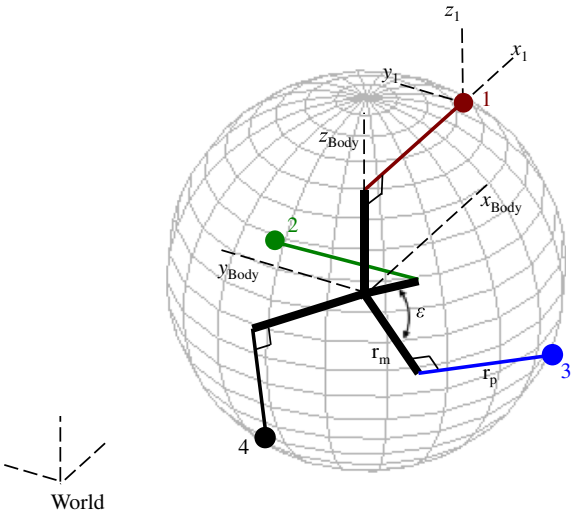

Fig. 3 Sketch of four-pendulum coordinate frames

The homogeneous standard rotation and translation matrices for the Body are $\boldsymbol{R}_\phi$, $\boldsymbol{R}_\theta$, $\boldsymbol{R}_\psi$, and $\boldsymbol{D}_{xy}$, with total transformation from Body to World of

$$ {}^W_B\boldsymbol{T} = \boldsymbol{D}_{xy}\boldsymbol{R}_\phi\boldsymbol{R}_\theta\boldsymbol{R}_\psi . \tag{1} $$

The sphere's position in the world is

$$ {}^W\boldsymbol{p}_S = {}^W_B\boldsymbol{T}\begin{bmatrix}0&0&0&1\end{bmatrix}^{\mathrm{T}} = \begin{bmatrix}x&y&0&1\end{bmatrix}^{\mathrm{T}} . \tag{2} $$

The ith pendulum frame is defined such that the x_i-axis is aligned with the pendulum arm and the z_i-axis is parallel to its rotation axis. As the pendulum rotates with angle α_i, the transformation from i to the motor's position is (using notation c and s for cosine and sine)

$$ \boldsymbol{T}_i = \begin{bmatrix} c\alpha_i & -s\alpha_i & 0 & r_p c\alpha_i \\ s\alpha_i & c\alpha_i & 0 & r_p s\alpha_i \\ 0 & 0 & 1 & r_m \\ 0 & 0 & 0 & 1 \end{bmatrix} . \tag{3} $$

The motors are mounted in a tetrahedral pattern defined by the tetrahedral angle$\varepsilon = \cos^{-1}\left(-1/3\right) \approx 109.5°$ and 120° rotations about the z-axis, represented by rotation matrices

$$ \boldsymbol{R}_\varepsilon = \begin{bmatrix} c\varepsilon & 0 & s\varepsilon & 0 \\ 0 & 1 & 0 & 0 \\ -s\varepsilon & 0 & c\varepsilon & 0 \\ 0 & 0 & 0 & 1 \end{bmatrix} , $$

$$ \boldsymbol{R}_{120} = \begin{bmatrix} c120° & -s120° & 0 & 0 \\ s120° & c120° & 0 & 0 \\ 0 & 0 & 1 & 0 \\ 0 & 0 & 0 & 1 \end{bmatrix} . \tag{4} $$

Therefore, the transformations for the four pendulums are

$$ \begin{aligned} {}^B_1\boldsymbol{T} &= \boldsymbol{T}_{i=1}, \\ {}^B_2\boldsymbol{T} &= \boldsymbol{R}_\varepsilon\boldsymbol{T}_{i=2}, \\ {}^B_3\boldsymbol{T} &= \boldsymbol{R}_{120}\boldsymbol{R}_\varepsilon\boldsymbol{T}_{i=3}, \\ {}^B_4\boldsymbol{T} &= \boldsymbol{R}^{\mathrm{T}}_{120}\boldsymbol{R}_\varepsilon\boldsymbol{T}_{i=4}. \end{aligned} \tag{5} $$

Pendulum i located at

$$ {}^W\boldsymbol{p}_i = {}^W_B\boldsymbol{T}\,{}^B_i\boldsymbol{T}\begin{bmatrix}0&0&0&1\end{bmatrix}^T = \begin{bmatrix}x_i&y_i&z_i&1\end{bmatrix}^T . \tag{6} $$

The system therefore has 9 generalized coordinates: the three Euler angles, the two translations, and the four pendulum angles:

$$ \boldsymbol{q} = [\phi, \theta, \psi, x, y, \alpha_1, \alpha_2, \alpha_3, \alpha_4]^T . \tag{7} $$

The translational velocities of the sphere and pendulums are the time derivatives of the $\boldsymbol{p}$'s above:

$$ {}^W\dot{p}_s = \begin{bmatrix}\dot{x}&\dot{y}&0&0\end{bmatrix}^T \tag{8} $$

$$ \begin{aligned} {}^W\dot{p}_i &= \frac{d}{dt}\left({}^W_B\boldsymbol{T}\,{}^B_i\boldsymbol{T}\begin{bmatrix}0&0&0&1\end{bmatrix}^T\right) \\ &= \begin{bmatrix}\dot{x}_i&\dot{y}_i&\dot{z}_i&0\end{bmatrix}^T . \end{aligned} \tag{9} $$

The mechanism is to be simulated in MATLAB, so it is advantageous to rewrite the ${}^W\dot{p}_i$ equation to eliminate time derivatives of functions. This can be done by using the chain rule:

$$ {}^W\dot{p}_i = \begin{bmatrix} \frac{\partial {}^W\boldsymbol{p}_i}{\partial q_1} & \frac{\partial {}^W\boldsymbol{p}_i}{\partial q_2} & \cdots & \frac{\partial {}^W\boldsymbol{p}_i}{\partial q_9} \end{bmatrix}\dot{q} . \tag{10} $$

The angular velocities of the sphere in World and Body coordinates are

$$ \begin{aligned} {}^W\boldsymbol{\omega}_s = \dot{\phi} + \dot{\theta} + \dot{\psi} &= \begin{bmatrix}0\\0\\\dot{\phi}\\0\end{bmatrix} + \boldsymbol{R}_\phi\begin{bmatrix}\dot{\theta}\\0\\0\\0\end{bmatrix} \\ &\quad + \boldsymbol{R}_\phi\boldsymbol{R}_\theta\begin{bmatrix}0\\0\\\dot{\psi}\\0\end{bmatrix} \\ &= \begin{bmatrix}\dot{\theta}c\phi + \dot{\psi}s\phi s\theta \\ \dot{\theta}s\phi - \dot{\psi}c\phi s\theta \\ \dot{\phi} + \dot{\psi}c\theta \\ 0\end{bmatrix} \\ &= \begin{bmatrix} 0 & c\phi & s\phi s\theta & 0 \\ 0 & s\phi & -c\phi s\theta & 0 \\ 1 & 0 & c\theta & 0 \\ 0 & 0 & 0 & 1 \end{bmatrix}\begin{bmatrix}\dot{\phi}\\\dot{\theta}\\\dot{\psi}\\0\end{bmatrix} , \end{aligned} \tag{11} $$

and

$$
\begin{aligned}
{}^{B}\boldsymbol{\omega}_{s} &= \boldsymbol{R}_{\psi}^{-1}\boldsymbol{R}_{\theta}^{-1}\begin{bmatrix}0\\0\\\dot{\phi}\\0\end{bmatrix}+\boldsymbol{R}_{\psi}^{-1}\begin{bmatrix}\dot{\theta}\\0\\0\\0\end{bmatrix}+\begin{bmatrix}0\\0\\\dot{\psi}\\0\end{bmatrix}\\
&= \begin{bmatrix} s\psi s\theta & c\psi & 0 & 0\\ c\psi s\theta & -s\psi & 0 & 0\\ c\theta & 0 & 1 & 0\\ 0 & 0 & 0 & 1\end{bmatrix}\begin{bmatrix}\dot{\phi}\\\dot{\theta}\\\dot{\psi}\\0\end{bmatrix}. \qquad (12)
\end{aligned}
$$

It is advantageous to define both – as shown later, the World form is needed for the constraint equations, while the Body form is used with the (Body-frame) inertia for the kinetic energy.

The relative angular velocity of pendulum i with respect to the sphere is

$$
{}^{B}\boldsymbol{\omega}_{i/s} = {}^{B}_{i}\boldsymbol{T}^{i}\,\omega_{i/s} = {}^{B}_{i}\boldsymbol{T}\begin{bmatrix}0 & 0 & \dot{\alpha}_i & 0\end{bmatrix}^{T}. \qquad (13)
$$

Therefore, the pendulum's total angular velocity is

$$
{}^{B}\boldsymbol{\omega}_{i} = {}^{B}\boldsymbol{\omega}_{s} + {}^{B}\boldsymbol{\omega}_{i/s}. \qquad (14)
$$

3.2 Equations of Motion: Lagrange Equations

The Lagrange equations of motion and generalized coordinates are

$$
L = K_{total} - U_{total}
$$

$$
\frac{d}{dt}\left(\frac{\partial L}{\partial \dot{q}_k}\right) - \frac{\partial L}{\partial q_k} = \sum_{i=1}^{n}\lambda_i a_{ik} + F_k \qquad (15)
$$

where $L$is the Lagrangian, $K_{total}$and U_{total} are the system's kinetic and potential energies, k corresponds to the generalized coordinate (1 to 9), n is the number of constraint equations, the λ's are the Lagrange multipliers for the constraints, the a's are the coefficient in the constraint equations for each generalized coordinate, and the F's are the nonconservative forces (friction, motor torques, etc.) on the generalized coordinates. Using the chain rule and rewriting following the method described in [26], the equations become

$$
\begin{aligned}
&\sum_{j=1}^{9}\left(\frac{d\left(\partial K \Big/ \partial \dot{q}_k\right)}{dq_j}\dot{q}_j + \frac{d\left(\partial K \Big/ \partial \dot{q}_k\right)}{d\dot{q}_j}\ddot{q}_j\right)\\
&-\frac{\partial K}{\partial q_k} + \frac{\partial U}{\partial q_k} = \sum_{i=1}^{n}\lambda_i a_{ik} + F_k \qquad (16)
\end{aligned}
$$

where j sums through the generalized coordinates. A third version is useful for control applications:

$$
\boldsymbol{M}(\boldsymbol{q})\,\ddot{q} + \boldsymbol{V}(\boldsymbol{q},\dot{q}) + \boldsymbol{G}(\boldsymbol{q}) = \sum_{j=1}^{n}\lambda_i a_j + \boldsymbol{F} \qquad (17)
$$

where $\boldsymbol{M}$ is the inertia matrix, $\boldsymbol{V}$ is the Coriolis and centripetal vector, and $\boldsymbol{G}$ is the gravity vector. The matrix and vectors have terms

$$
\begin{aligned}
\boldsymbol{M}_{kj}(\boldsymbol{q}) &= \frac{d\left(\partial K \Big/ \partial \dot{q}_k\right)}{d\dot{q}_j},\\
\boldsymbol{V}_k(\boldsymbol{q},\dot{q}) &= \sum\nolimits_{j=1}^{9}\left(\frac{d\left(\partial K \Big/ \partial \dot{q}_k\right)}{dq_j}\dot{q}_j\right) - \frac{\partial K}{\partial q_k},\\
\boldsymbol{G}_k(\boldsymbol{q}) &= \frac{\partial U}{\partial q_k}. \qquad (18)
\end{aligned}
$$

The mechanism has static mass M(shell, frame, electronics, motors, etc.) and moveable pendulum masses of m each. The translational ('_t') kinetic energies are

$$
K_{s\_t} = \frac{1}{2}{}^{W}\dot{p}_s^{T}M\,{}^{W}\dot{p}_s = \frac{1}{2}M\left(\dot{x}^2+\dot{y}^2\right) \qquad (19)
$$

$$
K_{i\_t} = \frac{1}{2}{}^{W}\dot{p}_i^{T}m\,{}^{W}\dot{p}_i = \frac{1}{2}M\left(\dot{x}_i^2+\dot{y}_i^2+\dot{z}_i^2\right). \qquad (20)
$$

The sphere has moment of inertia tensor $\boldsymbol{I}_s$ and rotational kinetic energy

$$
\begin{aligned}
K_{s\_r} &= \frac{1}{2}{}^{B}\boldsymbol{\omega}_s^{T}\boldsymbol{I}_s\,{}^{B}\boldsymbol{\omega}_s\\
&= \frac{1}{2}\left(I_{xx_s}\,{}^{B}\omega_x^2 + I_{yy_s}\,{}^{B}\omega_y^2 + I_{zz_s}\,{}^{B}\omega_z^2\right). \qquad (21)
\end{aligned}
$$

Each pendulum's inertia must be shifted to the motor via the Parallel Axis Theorem to define tensor ${}^{i}\boldsymbol{I}_i$ and rotational ('_r') kinetic energy

$$
{}^{i}\boldsymbol{I}_i = m\begin{bmatrix} Y_i^2+Z_i^2 & -X_iY_i & -X_iZ_i & 0\\ -X_iY_i & X_i^2+Z_i^2 & -Y_iZ_i & 0\\ -X_iZ_i & -Y_iZ_i & X_i^2+Y_i^2 & 0\\ 0 & 0 & 0 & 0\end{bmatrix} \qquad (22)
$$

$$
K_{i\_r} = \frac{1}{2}{}^{B}\boldsymbol{\omega}_i^{T}\left({}^{B}_{i}\boldsymbol{T}\cdot{}^{i}\boldsymbol{I}_i\cdot{}^{B}_{i}\boldsymbol{T}^{T}\right){}^{B}\boldsymbol{\omega}_i \qquad (23)
$$

where $X_i = r_p c\alpha_i$, $Y_i = r_p s\alpha_i$, and $Z_i = r_m$. The total kinetic energy is

$$
K_{total} = K_{s\_t} + K_{s\_r} + \sum_{i=1}^{4}\left(K_{i\_t} + K_{i\_r}\right) \qquad (24)
$$

The potential energies are

$$U_s = \begin{bmatrix} 0 & 0 & Mg & 0 \end{bmatrix} \cdot {}^W\boldsymbol{p}_S = 0, \tag{25}$$

$$U_i = \begin{bmatrix} 0 & 0 & mg & 0 \end{bmatrix} \cdot {}^W\boldsymbol{p}_i = mgz_i, \tag{26}$$

with total

$$U_{total} = U_s + \sum_{i=1}^{4} U_i. \tag{27}$$

The R-radius sphere is assumed to roll without slipping, implementing two nonholonomic constraint equations ($n = 2$):

$$f_1 = \dot{x} - R \cdot {}^W\omega_{y_s} = 0, \tag{28}$$

$$f_2 = \dot{y} + R \cdot {}^W\omega_{x_s} = 0. \tag{29}$$

Defining rolling damping as b_{roll}, motor damping as b_{motor}, and motor torques as τ_i, the constraint coefficients and nonconservative forces can be modeled as

$$\boldsymbol{a}_1 = \begin{bmatrix} \partial f_1 / \partial \phi \\ \partial f_1 / \partial \theta \\ \partial f_1 / \partial \psi \\ 1 \\ 0 \\ 0 \\ 0 \\ 0 \\ 0 \end{bmatrix}, \boldsymbol{a}_2 = \begin{bmatrix} \partial f_2 / \partial \phi \\ \partial f_2 / \partial \theta \\ \partial f_2 / \partial \psi \\ 0 \\ 1 \\ 0 \\ 0 \\ 0 \\ 0 \end{bmatrix},$$

$$\boldsymbol{F} = \begin{bmatrix} 0 \\ 0 \\ 0 \\ -b_{roll} \\ -b_{roll} \\ \tau_1 - b_{motor} \\ \tau_2 - b_{motor} \\ \tau_3 - b_{motor} \\ \tau_4 - b_{motor} \end{bmatrix}. \tag{30}$$

The four-pendulum equations of motion have been simulated in MATLAB. To simulate the nine coordinate and two constraint equations, the multipliers are solved for using the x and y equations:

$$\begin{aligned} \lambda_1 &= \boldsymbol{M}_4(\boldsymbol{q})\ddot{\boldsymbol{q}} + \boldsymbol{V}_4(\boldsymbol{q}, \dot{q}) + \boldsymbol{G}_4(\boldsymbol{q}) - F_4 \\ \lambda_2 &= \boldsymbol{M}_5(\boldsymbol{q})\ddot{\boldsymbol{q}} + \boldsymbol{V}_5(\boldsymbol{q}, \dot{q}) + \boldsymbol{G}_5(\boldsymbol{q}) - F_5 \end{aligned} \tag{31}$$

where the 4 and 5 subscripts signify rows of the matrices and vectors. The multipliers are then substituted back into the remaining seven Lagrange equations (k signifies row, from 1 to 3 and 6 to 9):

$$\begin{aligned} &(\boldsymbol{M}_k - \boldsymbol{a}_{1k}\boldsymbol{M}_4 - \boldsymbol{a}_{2k}\boldsymbol{M}_5)\ddot{\boldsymbol{q}} \\ &+ (\boldsymbol{V}_k - \boldsymbol{a}_{1k}\boldsymbol{V}_4 - \boldsymbol{a}_{2k}\boldsymbol{V}_5) + (\boldsymbol{G}_k - \boldsymbol{a}_{1k}\boldsymbol{G}_4 - \boldsymbol{a}_{2k}\boldsymbol{G}_5) \\ &= (F_k - \boldsymbol{a}_{1k}\boldsymbol{F}_4 - \boldsymbol{a}_{2k}\boldsymbol{F}_5). \end{aligned} \tag{32}$$

The two constraint equations are differentiated (again using the chain rule):

$$\begin{aligned} \frac{df_1}{dt} = \frac{d}{dt}\left(\boldsymbol{a}_1^T\dot{q}\right) &= \ddot{q} + \left[\frac{\partial \boldsymbol{a}_1^T}{\partial \boldsymbol{q}}\dot{q}\right]^T \dot{q} \\ &= \boldsymbol{a}_1^T\ddot{q} + \dot{q}^T\frac{\partial \boldsymbol{a}_1}{\partial \boldsymbol{q}}\dot{q} = 0 \end{aligned} \tag{33}$$

$$\frac{df_2}{dt} = \boldsymbol{a}_2^T\ddot{q} + \dot{q}^T\frac{\partial \boldsymbol{a}_2}{\partial \boldsymbol{q}}\dot{q} = 0$$

The differentiation is a standard method (e.g., [27]) and is needed to make the new inertia matrix full rank. These equations are in Eq. 18 form — for example,

$$\left[\boldsymbol{a}_1^T\right]\ddot{q} + \left(\dot{q}^T\frac{\partial \boldsymbol{a}_1}{\partial \boldsymbol{q}}\dot{q}\right) + (0) = 0 + 0 \tag{34}$$

— and can be combined with the seven remaining Lagrange equations. With these modifications, the simulation takes the resulting nine equations, inverts the new inertia matrix, and solves for $\ddot{q}$.

4 Simulation Results

The mechanism dynamics have been simulated in MATLAB for various initial conditions and torques using normalized values of $M = 1.0$ (modeled as a homogenous sphere), $m = 0.25$ (modeled as a point mass), and R=1. In the results shown here, the rolling damping and motor damping are assumed zero. Due to the equations' nonholonomic nature, the simulation is susceptible to ill-conditioned configurations that result in singularities in the inverted inertia matrix, and results show slight numerical errors in energy conservation; both limitations are similar to those seen by other authors (e.g., [5, 20]). The following three examples, however, demonstrate the validity of the equations and mechanism, and the simulation's usefulness for future analysis and control schemes testing.

4.1 Free Response

Figure 4 shows a sample free-response path and state variables (i.e., no applied torques). For this simulation, the mechanism was given an initial rolling velocity towards positive x:

$$\dot{q} = [0, 0, -2\pi, 2\pi, 0, 0, 0, 0, 0]^T . \tag{35}$$

The results show the mechanism (and simulation) behaving as expected. The sphere rolls in the positive x direction with wobbling due to the free-spinning pendulums and the inherent wobbliness of spherical robots (discussed later). The sphere positions, sphere angles, and pendulum angles are shown in Fig. 4b; the pendulum angles are increasing as the sphere rotates but the pendulums do not.

4.2 Single-Pendulum Response

Figure 5 also shows the mechanism and simulation behaving as expected. The figure shows a sample single-torque response path, with plots of state variables and energy in the system. For this simulation, the initial velocities were zero but a constant (normalized) torque was applied to one pendulum (colored red in the figure):

$$\boldsymbol{F} = [0, 0, 0, 0, 0, -1, 0, 0, 0]^T . \tag{36}$$

As expected, the mechanism rolls towards negative x due to the applied torque and towards positive $y$due to the unbalanced weight of the other three pendulums. The simulation did not apply any control

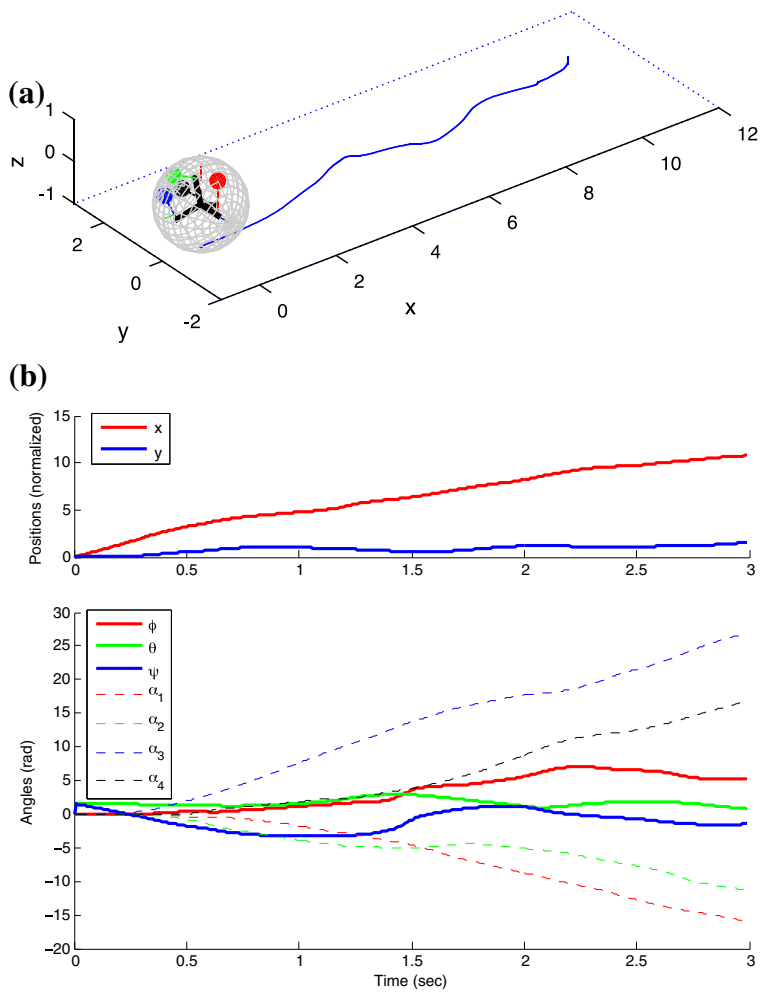

Fig. 4 Simulation results showing a normalized free-response path due to an initial rolling velocity. **a** Initial position and subsequent path of sphere. **b** State variables

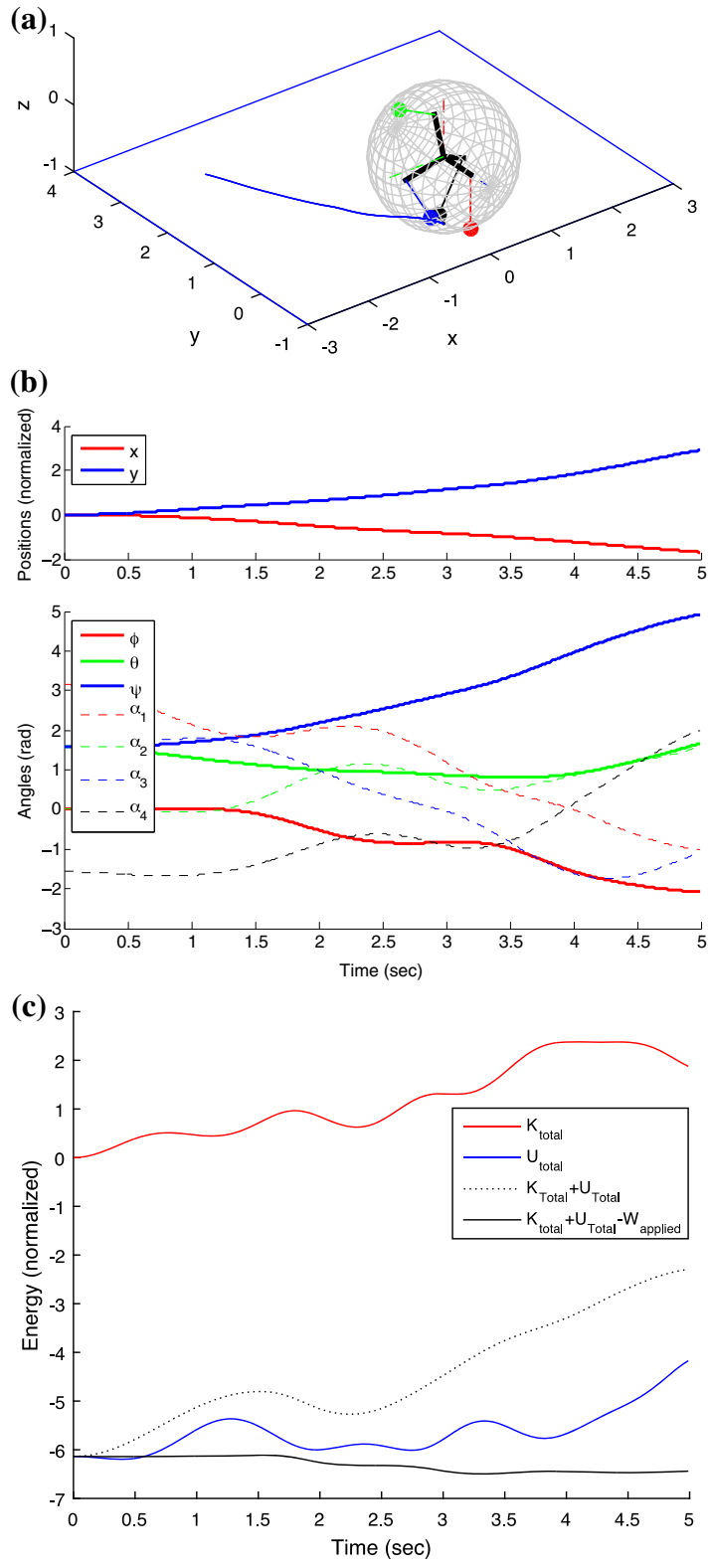

Fig. 5 Simulation results showing **a** path and **b** state variables, **c** energy when torque is applied to one pendulum

to the other pendulums or towards maintaining a desired rolling velocity. The energy plot shows that the total energy in the system is increasing due to the applied torque, but once the work associated with the torque ($W_{applied}$) is removed, the remaining energies remain relatively constant (within 3.2 %). As mentioned previously, this slight fluctuation in the simulation's energy is expected and is due to numerical rounding and matrix-inversion approximations.

4.3 Double-Pendulum Response

Results from a third example simulation are shown in Fig. 6. Here, the simulation applied constant torques to two of the pendulums (colored blue and black in the figure),

$$\boldsymbol{F} = [0, 0, 0, 0, 0, 0, 0, 0, -1, -1]^T . \tag{37}$$

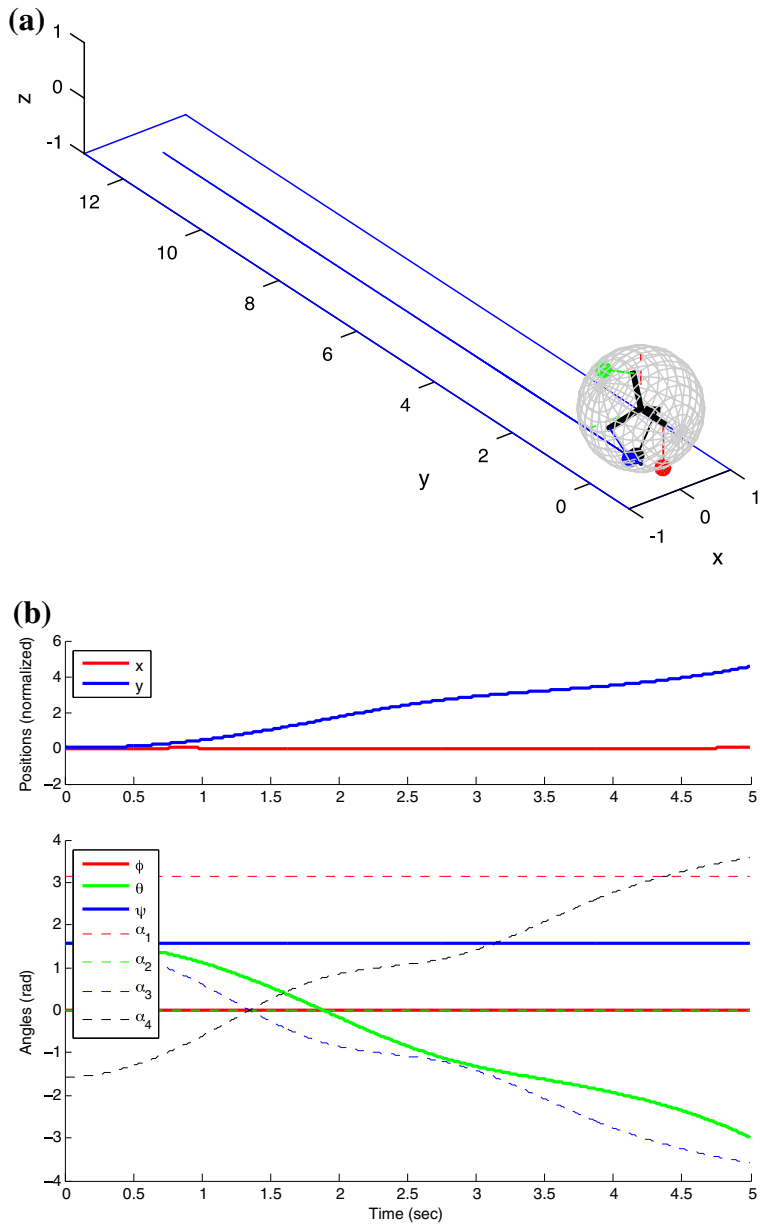

Fig. 6 Simulation results showing **a** path and **b** state variables when torque is applied to two pendulums

causing the sphere to roll towards positive y. Because of the symmetry of both the actuated and the free-spinning pendulums, the path is a straight line. However, the speed along the path is not constant, as shown by the slope of the y plot. The simulation did not attempt to control that speed.

5 Comparison to Existing Center-of-mass Designs

This section compares the new four-pendulum mechanism to existing center-of-mass spherical robot designs, here called the single-pendulum, the four (tetrahedral) sliders, and the cable-mass designs. The comparison is made on three aspects of the mechanisms, as discussed below and summarized in Table 1. The terminology and comparisons used are beneficial for determining each mechanism's strengths and weaknesses with regards to the others.

5.1 Directionality Comparison

The first comparison is on the directionality of the mechanism. Here, directionality is meant as the number of directions the sphere can roll instantly from rest. It is meant as a general term rather than a technical one. Ideally, a spherical robot should be able to roll in any direction instantly, as this provides navigational advantages in complex environments. In that regard, the four-pendulum, four sliders, and cable-mass designs are omnidirectional, while the more common single-pendulum design is not.

5.2 Torque Arm Comparison

The second comparison is on the theoretical normalized torque arm. When a mechanism shifts its center of mass from its geometric center, the mass creates a rolling torque proportional to its distance. That distance, or torque arm, can be modeled as the percentage of the sphere radius, assuming point masses and no static mass:

$$r_\tau = \frac{\text{horizontal distance to CoM}}{R} \cdot 100\ \%. \tag{38}$$

For center of mass designs, $0 < r_\tau < 100\ \%$. This is an ideal mechanism calculation, since in actuality the robot's shell, frame, and electronics create a static mass that reduces the effective torque arm (e.g., 50–67 % [20]).

Existing designs have either large or small maximum torque arms. Using this metric, the single-pendulum design has a theoretical 100 % torque arm since the pendulum's mass can be moved out to the sphere's radius at any angle (<100 %). The cable mass design has a similar maximum, although it is not at any angle (<100 %) – the mass cannot extend past the bisection line between any two cable mounts. On the other hand, the four-slider design has a much more restricted torque arm – simulations show a center of mass envelope of a polyhedron with maximum torque arm ranging from 20–29 %.

The proposed four-pendulum mechanism has a maximum torque arm length between those of the existing designs. If the four pendulums are equal, then its center of mass can be calculated as the average of the positions and the envelope of possible locations is a truncated sphere. From the simulation, the maximum torque arm ranges from 56–67 %, depending on the angle. That is, the four-pendulum design can ideally generate torques equivalent to up to two-thirds of its radius.

Table 1 Comparison of several theoretical center-of-mass designs

Design	Single pendulum	Four sliders	Cable mass	Four pendulums
Directionality	Steered	Omni	Omni	Omni
Torque arm, r_T	<100 %	<29 %	<100 %	<67 %
Eccentricity, e	100 %	0–20 %	0, 100 %	36–100 %

5.3 Eccentricity Comparison

The third comparison between designs is the eccentricity of the robot's rotational moment of inertia about its center. A general three-dimensional body has an inertia ellipsoid representing its rotational inertia in any direction. The eccentricity of the ellipse (mathematically, "first eccentricity") is defined here as

$$e = \sqrt{1 - \frac{I_{\text{minor}}^2}{I_{\text{major}}^2}} \cdot 100\ \%, \tag{39}$$

where I_{major} and I_{minor} are the robot's principal moments of inertia about the ellipse's major and minor axes.

A well-known challenge of spherical robots is that their inertia ellipses are not spherical ($I_{major} > I_{minor}$). As the robot rolls, angular momentum is conserved. However, the robot's angular inertia is not constant, and so the angular velocity varies resulting in wobbling of the sphere. Thus, having a mechanism with little eccentricity (i.e., more homogeny) is advantageous since it results in less wobble.

Existing designs have either high or low eccentricity. A theoretical single-pendulum or cable-mass design has one point mass, and thus an inertia ellipse collapsed into a line. Their eccentricity is always 100 % (unless, in the cable-mass design, the mass is at the center), resulting in wobbling. In this regard, the four-slider design is better. Simulation shows that the four-slider design has an eccentricity of <20 %; the four-slider design is less prone to wobbling.

Similar to the torque arm comparison, the new four-pendulum design's eccentricity is between the existing designs' eccentricities. The four-pendulum's eccentricity varies depending on the configuration of the pendulums, and ranges from 36 % to 100 %, with an average of 84 %. The 36 % occurs when the four pendulums are pointing in various directions, while the 100 % occurs when they are paired at opposite sides of the sphere. Thus, the four-pendulum design is less prone to wobble than the single-pendulum and cable-mass designs, but more prone than the four-sliders design.

5.4 Comparison Summary

As noted, these comparisons are based on theoretical mechanisms. A physical robot will have numbers that are more conservative. The four-pendulum prototype is a successful proof-of-concept robot that is not optimized for minimal static mass, but may be useful as an example. As mentioned previously, it has a static and dynamic masses of 2.6 kg and 1.6 kg; in Chase and Pandya's [1] terminology, it has a power factor of 0.615. The mechanism's theoretical maximum torque arm is calculated as 56–67 %; the prototype's effective maximum is closer to 20 %. On the other hand, the prototype's eccentricity is better because of the static mass. The mechanism's theoretical eccentricity is 36–100 %, with an average of 84 %; the prototype's eccentricity is 30–92 %, with an average of 73 %.

6 Conclusions and Future Work

The proposed four-pendulum center-of-mass spherical robot is a novel and successful mechanism. The nonholonomic equations of motion have been mathematically derived and numerically simulated, showing expected behaviors. The mechanism is also a balance of existing center-of-mass designs in that it is omnidirectional, has torque arm around two-thirds of the sphere's radius, and inertia eccentricity of an average 84 %. The mechanism has been successfully implemented on a physical prototype that demonstrates the validity of the four-pendulum design.

The mechanism and equations show promise for future work. For example, the Euler-angle representation used here is known for its ill-conditioning near "gimbal lock" orientations. One possible improvement is to derive and simulate the equations of motion using quaternions rather than Euler-angles. Furthermore, the simulation behaves as expected but the examples show the sphere does not roll with controlled heading or speed. A next step is to apply drive-velocity and path-following control schemes to the four-pendulum mechanism. In addition, the prototype is remote-controllable, but not autonomous; future work includes adding global position feedback and autonomous control. Finally, the omnidirectionality of the four-pendulum design complicates the use of orientation-dependent sensors such as video cameras and ultrasonic position sensors since there is no consistent roll axis. An unanswered research question is how to apply, fuse, or simulate such sensors on an omnidirectional spherical robot.

Acknowledgments This work was funded in part by the Central Michigan University FRCE Grant #48868.

References

1. Chase, R., Pandya, A.: A review of active mechanical driving principles of spherical robots. Robotics **1**, 3–23 (2012)
2. Crossley, V.A.: A literature review of the design of spherical rolling robots. Department of Mechanical Engineering, Carnegie Mellon University, Pittsburgh (2006)

3. Armour, R.H., Vincent, J.F.V.: Rolling in nature and robotics: a review. J. Bionic Eng. **3**(4), 12, 195–208 (2006)
4. Seeman, M., Broxvall, M., Saffiotti, A., Wide, P.: An autonomous spherical robot for security tasks. In: IEEE Conference on Computational Intelligence for Homeland Security and Personal Safety (2006)
5. Hogan, F.R., Forbes, J.R., Barfoot, T.D.: Rolling stability of a power-generating tumbleweed rover. J. Spacecr. Rocket. **51**(6), 1895–1906 (2014)
6. Hernandez, J.D., Barrientos, J., del Cerro, J., Barrientos, A., Sanz, D.: Moisture measurement in crops using spherical robots. Industrial Robot: An International Journal **40**(1), 59–66 (2013)
7. Li, M., Guo, S., Hirata, H., Ishihara, H.: Design and performance evaluation of an amphibious spherical robot. Robot. Auton. Syst. **64**, 21–34 (2015)
8. Michaud, F., Laplante, J.-F., Larouche, H., Duquette, A., Caron, S., Letourneau, D., Masson, P.: Autonomous spherical mobile robot for child-development studies. IEEE Trans. Syst. Man Cybern. **35**(4), 471–479 (2005)
9. Bhattacharya, S., Agrawal, S.K.: Spherical rolling robot: a design and motion planning studies. IEEE Trans. Robot. Autom. **16**(6), 835–9 (2000)
10. Joshi, V.A., Banavar, R.N., Hippalgaonkar, R.: Design and analysis of a spherical mobile robot. Mech. Mach. Theory **45**(2), 130–136 (2010)
11. Gajamohan, M., Muehlebach, M., Widmer, T., D'Andrea, R.: The Cubli: a reaction wheel based 3D inverted pendulum. In: European Control Conference (2013)
12. Sugiyama, Y., Shiotsu, A., Yamanaka, M., Hirai, S.: Circular/spherical robots for crawling and jumping. In: IEEE International Conference on Robotics and Automation (2005)
13. Wait, K.W., Jackson, P.J., Smoot, L.S.: Self locomotion of a spherical rolling robot using a novel deformable pneumatic method. In: IEEE International Conference on Robotics and Automation (2010)
14. Artusi, M., Potz, M., Aristizabal, J., Menon, C., Cocuzza, S., Debei, S.: Electroactive elastomeric actuators for the implementation of a deformable spherical rover. IEEE/ASME Trans. Mechatron. **16**(1), 50–57 (2011)
15. Lux, J.: Alternative Way of Shifting Mass to Move a Spherical Robot. Tech Rep., NASA's Jet Propulsion Laboratory, June (2005)
16. Halme, A., Schonberg, T., Wang, Y.: Motion control of a spherical mobile robot. In: 4Th International Workshop on Advanced Motion Control, pp. 259–264 (1996)
17. Bicchi, A., Balluchi, A., Prattichizzo, D., Gorelli, A.: Introducing the Sphericle: an experimental testbed for research and teaching in Nonholonomy. In: IEEE International Conference on Robotics and Automation, pp. 2620–2625 (1997)
18. Alves, J., Dias, J.: Design and control of a spherical mobile robot. Journal of Systems and Control Engineering **217**, 457–467 (2003)
19. Michaud, F., Caron, S.: Roball, the rolling robot. Auton. Robot. **12**(2), 211–222 (2002)
20. Schroll, G.C.: Dynamic Model of a Spherical Robot from First Principles. Master's Thesis, Colorado State University, Summer (2010)
21. Ghanbari, A., Mahboubi, S., Fakhrabadi, M.: Design, dynamic modeling and simulation of a spherical mobile robot with a novel motion mechanism. In: IEEE/ASME International Conference on Mechatronics and Embedded Systems and Applications (MESA), pp. 434–439 (2010)
22. Yoon, J.-C., Ahn, S.-S., Lee, Y.-J.: Spherical robot with new type of two-pendulum driving mechanism. In: 15Th IEEE International Conference on Intelligent Engineering Systems (INES), IEEE, pp. 275–279 (2011)
23. Javadi A., A.H., Mojabi, P.: Introducing glory: a novel strategy for an omnidirectional spherical rolling robot. J. Dyn. Syst. Meas. Control. **126**(3), 678–83 (2004)
24. Sang, S., Zhao, J., Hao, W., Qi, A.: Modeling and simulation of a spherical mobile robot. Computer Science and Information Systems **7**(1) (2010)
25. Tomik, F., Nudehi, S., Flynn, L.L., Mukherjee, R.: Design, fabrication and control of SpheRobot: a spherical mobile robot. J. Intell. Robot. Syst. **67**(2), 117–131 (2012)
26. Karadogan, E., Williams, R.L.: The Robotic Lumbar Spine: Dynamics and Feedback Linearization Control. Computational and Mathematical Methods in Medicine, vol. 2013 (2013)
27. Murray, R., Li, Z., Sastry, S.S.: A Mathematical Introduction to Robotic Manipulation. CRC Press (1994)

Brian P. DeJong is an Associate Professor of Mechanical Engineering in the School of Engineering and Technology at Central Michigan University. He received a M.S. and Ph.D. in Mechanical Engineering from Northwestern University with research in robotics. His current research is in mobile robots (spherical, soundlocalization), teleoperation (improved interfaces), and engineering education.

Ernur Karadogan is an Assistant Professor of Mechanical Engineering in the School of Engineering & Technology at Central Michigan University, Mt. Pleasant, MI. He received his B.S. degree in Aerospace Engineering in 2000 from Middle East Technical University (METU), Ankara, Turkey, and his M.S. and Ph.D. degrees both in Mechanical Engineering from Ohio University (OU), Athens, Ohio in 2005 and 2011, respectively. His Ph.D. work was concentrated on the design of a cable-actuated robotic lumbar spine to be used as a palpatory training and assessment device for medical students. Formerly, he worked as a research scientist in the Fluid Mechanics Laboratory at the National Metrology Institute (TUBITAK-UME), Gebze-Kocaeli, Turkey from 2001 to 2003; as a research associate in the Mechanical Engineering Department at OU from 2005 to 2013; as an assistant professor in the Mechanical Engineering Department at the University of Texas Rio Grande Valley (formerly the University of Texas-Pan American), Edinburg, Texas between 2013 and 2015. His research interests include: Robotics, Haptics, Dynamic Systems & Control, Simulations in Virtual Environments, and Biomechanics.

Kumar Yelamarthi received his Ph.D. and M.S degree from Wright State University in 2008 and 2004. He is currently an Associate Professor of Electrical & Computer Engineering at Central Michigan University. His research interest is in the areas of Wireless Sensor Networks, Internet of Things, mobile robotics, computer vision, embedded systems, and engineering education. He has published over 90 articles in archival journals and conference proceedings in these areas. He served as PI, co-PI, and senior personnel in several externally funded grants from organizations such as NSF, NASA, and the regional industry. He is an elected member of Tau Beta Pi engineering honor society, and Omicron Delta Kappa national leadership honor society, and a senior member of IEEE.

James Hasbany is a graduate student pursuing his Masters of Science in Engineering at the School of Engineering and Technology at Central Michigan University. He has served in both Research and Teaching assistantships. He received a B.S. in Mechanical Engineering from Central Michigan University. His current research area is in spherical robots.